

Morphology control of Si₂Te₃ nanostructures synthesized by CVD

Keyue Wu^{1,3} · Jingbiao Cui²

Received: 16 October 2017 / Accepted: 21 April 2018 © Springer Science+Business Media, LLC, part of Springer Nature 2018

Abstract

As a silicon-based chalcogenide, Si_2Te_3 has recently attracted attentions as an emerging layered two-dimensional (2D) material. In this study, various Si_2Te_3 nano-structures, including vertical, titled, and horizontal plates, nanotapers, and nanowires were grown by controlling the growth conditions in a chemical vapor deposition. The Si_2Te_3 nanotapers and nanowires were synthesized with Au as a catalyst while only nanoplates and microplates were obtained without catalysts on the substrates. The microplates were found to be composed of multiple nanoplates overlapping with each other. Vapor–Solid model is proposed to dominate the growth of the nanotapers while Vapor-Liquid-Solid is dominant process for the growth of nanowires. The different morphologies of the Si_2Te_3 nanostructures may find potential applications in electronics and optoelectronics.

1 Introduction

As an emerging silicon-based semiconductor, silicon telluride ($\mathrm{Si_2Te_3}$) exhibits a strong optical response which may have potential applications in near infrared photodetectors, light emitting diodes, and energy storage devices [1]. $\mathrm{Si_2Te_3}$ exhibits a layered, trigonal crystal structure in space group $P\bar{3}1c$ with lattice constants a = 7.429 and c = 13.471 Å [2]. The Te atoms form an h.c.p lattice and the Si atoms appear to form dumb-bells between Te layers [3]. The crystals show easy cleavage perpendicular to the c axis, due to a weak bonding between those Te layers where no Si atoms are built in.

Most investigations on Si₂Te₃ were focused on bulk materials and performed 50 years ago [4–8]. The bulk Si₂Te₃ was reported to be a p-type semiconductor with indirect and direct electronic bands [4]. Zwick and Rieder investigated the optical absorption properties of bulk Si₂Te₃ and yielded a direct band-gap energy of 2.13 eV at room temperature and

2.34 eV at 4.2 K [5]. Ziegler and Birkholz investigated the photoelectric properties of bulk Si₂Te₃, and their photocurrent measurements showed that the maximum absorption was observed at 2.2 eV with a shoulder at 1.9 eV and another maximum at 1 eV [6].

Recently, several groups also studied the properties of Si₂Te₃ [9–12]. For example, Shen et al. reported a theoretical investigation showing the tunable the band gap and band structure of Si₂Te₃ with different orientations of Si dimmers [9]. Juneja et al. reported that the n-doped Si₂Te₃ exhibited a thermal conductivity below 2 W/mK and an unprecedented ZT of 1.86 at 1000 K by theoretical calculations [10].

Over the past decades, one-dimensional (1D) nanostructures of various materials and of different morphologies have been successfully synthesized. Nanowires (NWs) are anisotropic in shape and have been explored in many applications including nanoelectronics [13, 14], nanophotonics [15, 16], biosensors [17], thermoelectrics [18, 19], and energy conversion [20]. In additional, the two-dimensional (2D) nanostructures with tunable size, morphology, phase, as well as crystallographic orientation often exhibit distinct physical and chemical properties and are attractive for today's nanotechnology development [21–25]. Designing, controlling, and rational growth of 1D and 2D nano-architectures with complex structure configurations therefore play a central role for future applications in this field.

As a new one and two-dimensional functional material, Si₂Te₃ nanoplates and ribbons were recently synthesized by chemical vapor deposition [1], which has stimulated a great interest to revisit this silicon based semiconductor.

Published online: 28 April 2018



[⊠] Keyue Wu wukeyue@wxc.edu.cn

College of Electrical and Photoelectronic Engineering, West Anhui University, Lu'an 237012, Anhui, People's Republic of China

Department of Physics and Materials Science, University of Memphis, Memphis, TN 38152, USA

Research Center of Atoms Molecules and Optical Applications, West Anhui University, Lu'an 237012, Anhui, People's Republic of China

Recently, we investigated the temperature dependent photoluminescence of 2D Si₂Te₃ nanoplates synthesized by a CVD method [26].

Here, we report the synthesis of Si₂Te₃ nanoplates, nanotapers and nanowires by a CVD process. The morphology and structure of the obtained samples were characterized by various techniques. The growth mechanisms of microplates and nanotapers were proposed and the effects of growth conditions such as substrate temperature and time were studied. This work suggests that 1D and 2D Si₂Te₃ nanostructures can be achieved by a controlled CVD growth for future applications. These nanostructures have potential applications in memory devices, field emission, optoelectronics.

2 Experimental details

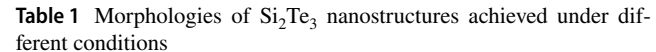
Tellurium (30 mesh, 99.997%) and silicon (325 mesh, 99%) powders were purchased from Aldrich and used as source materials for $\mathrm{Si_2Te_3}$ nanostructures preparation. Both Te and Si powders were placed in a ceramic crucible and loaded into a high temperature tube furnace. $\mathrm{SiO_2/Si}$ and Au coated $\mathrm{SiO_2/Si}$ substrates (The thickness of Au film is from 40 to 80 nm) were placed downstream of gas flow in the furnace. The quartz tube was first evacuated and then introduced with high purity nitrogen gas to maintain a pressure at 9.12 Torr. The nitrogen flow rate was set at 15 sccm by a mass flow controller. The furnace was then heated to 850 °C at a heating rate of 20 °C/min. The growth was conducted from 550 to 650 °C and allowed for a total time of 3–5 min, and then the ceramic crucible and substrates were cooled down to room temperature.

The morphology of the Si_2Te_3 nanowires was analyzed with a scanning electron microscopy (SEM). The crystal structure was characterized by X-ray diffraction (XRD) with Cu Ka radiation (λ =1.54 Å). Raman spectroscopy was measured by using a DXR Raman microscope with an excitation laser of 532 nm and 2 mW power.

3 Results and discussions

In the synthesis of ${\rm Si}_2{\rm Te}_3$ nanoplates, control over the morphology of the samples can be achieved by tuning the substrates temperature. Table 1 provides a summary of the growth morphology, growth conditions, substrate temperature range, growth time, and the use of catalysts.

Figure 1a shows the vertically aligned Si_2Te_3 nanoplates grown at 650 °C. The size of the nanoplates is about 1–2 micrometers with thickness of tens to hundreds of nanometers. The size, thickness, and orientation may vary, depending on the growth condition and time. With the decrease of the substrate temperature, vertically aligned Si_2Te_3

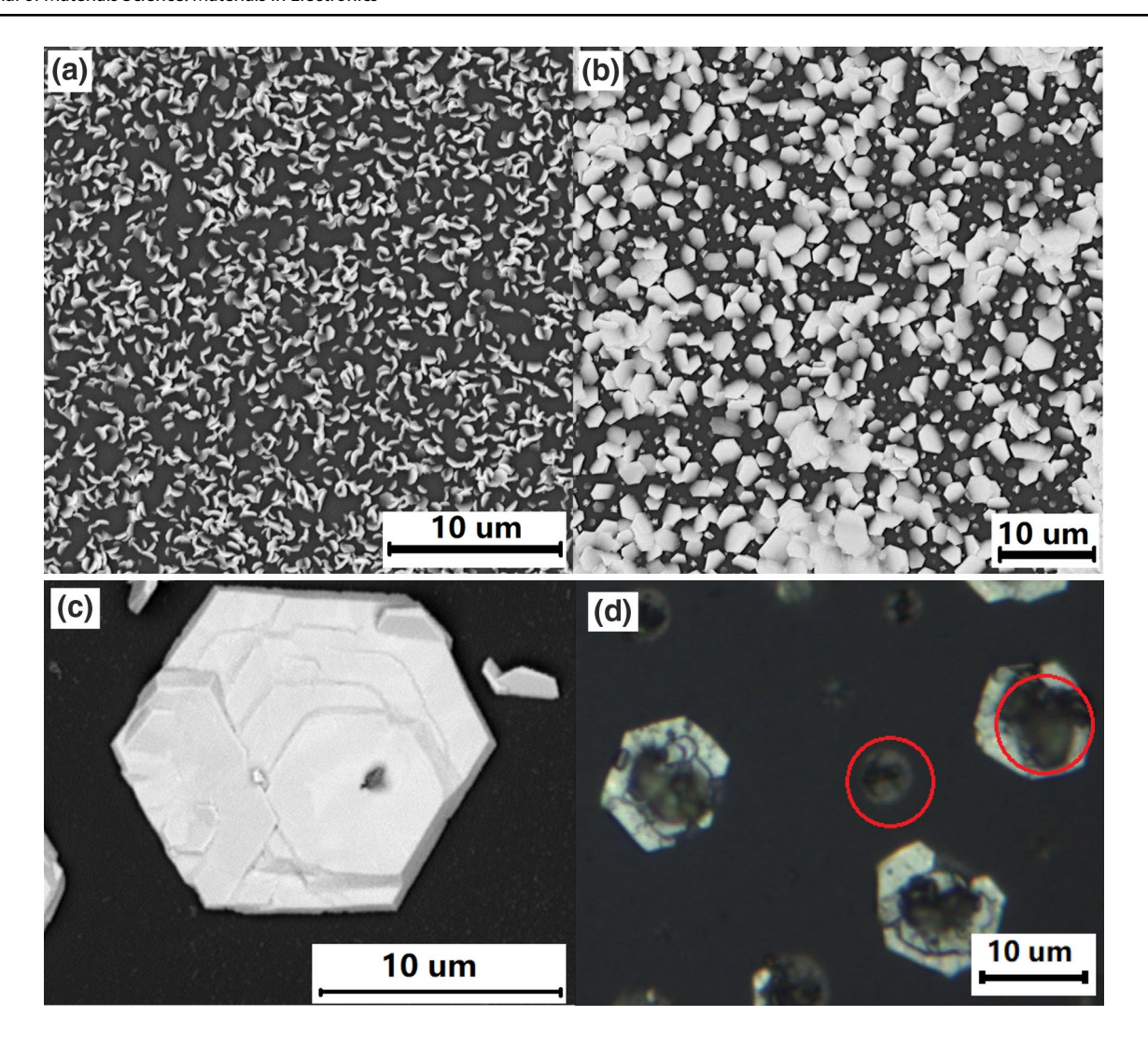


Growth morphology	Si/Te source temperature (°C)	Substrate temperature (°C)	Catalysts	Growth time (min)
Vertical nano- plates	850	650	None	3–5
Titled nano- plates	850	600	None	3–5
Flat plates	850	550	None	3–5
Nanotapers	850	580	Au	3–4
Nanowires	850	600	Au	4

nanoplates change to title nanoplates as shown in Fig. 1b. The average size of these nanoplates is larger than those vertical nanoplates. Further decreasing the substrate temperature to $550\,^{\circ}$ C, the size of the nanoplates continues to increase up to $10\,\mu m$ but flat plates as shown in Fig. 1c. The growth of the flat plates is consistent with the observations by Keuleyan et al. [1]. It can be seen from Fig. 1c that the large Si_2Te_3 nanoplates are composed of several small nanoplates stacking over each other. By changing the temperature, the different morphologies of Si_2Te_3 nanoplates were obtained with the same conditions for the sources.

Figure 2 shows the SEM images of Si₂Te₃ nanotapers and nanowires grown under similar conditions as the nanoplates but on the Au-coated substrates. Figure 2a shows the growth of conical structures of Si₂Te₃, which were obtained under 580 °C for about 4 min. The structures have thick bottom about 3 µm in diameter and sharp tips at the top. One can see that there are round caps on each of the cones, which are the Au catalysts. This seems to suggest that the growth at the tip of the structure is faster than the horizontal direction due to the presence of the catalysts [27]. From the inset of Fig. 2a, the tapered structures are formed by stacking of nanoplatelets along the vertical direction. The energy dispersive X-ray (EDX) mapping of Si₂Te₃ nanoplates were studied in our previous work [26], which confirmed the ratio of Si:Te as 2:3. The same composition was also obtained on the Si₂Te₃ nanowires reported in this study. This growth mode implies that VLS may be responsible for the vertical growth but the horizontal growth is still dominated at the bottom. Figure 2b shows an SEM image of Si₂Te₃ nanowires grown at the substrate temperature of 600 °C for 4 min. The nanowires with length up to 50 µm and diameter of hundred nanometers are obtained. The thickness of the nanowires is very uniform in contrast with the nanocones. Again Au catalysts are seen on the tips of the nanowires. The inset of Fig. 2b shows an individual nanowire with Au on the tip. The presence of a gold nanoparticle at the end of the nanowire suggests the VLS mechanism dominates the growth process, in which the gold catalyst induces the nucleation and growth of the





 $\textbf{Fig. 1} \quad \text{SEM and optical images of } Si_2Te_3 \text{ nanoplates. } \textbf{a} \text{ vertically alighned nanoplates; } \textbf{b} \text{ nanoplates growth with a titled angle; } \textbf{c} \text{ flat plates; } \text{and } \textbf{d} \text{ optical image of flat plates}$

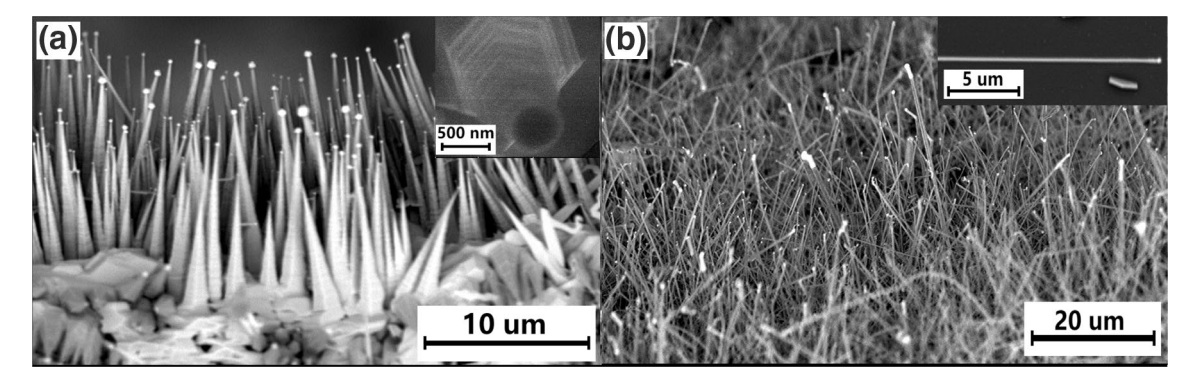


Fig. 2 SEM images of Si_2Te_3 nanotapers (a) and nanowires (b) grown at different temperatures

nanowires [28]. The other noble metals such as Pt, Ag, etc. were also tried to use as catalyst, which did not show success growth of Si₂Te₃ nanowires.

Figure 3 shows the XRD and Raman spectra of Si₂Te₃ nanoplates and nanowires. The XRD patterns shown in Fig. 3a reveal a very strong (004) diffraction peak of Si₂Te₃ at 26.5° along with a few other weak peaks at 27.5°, 36.1°, 40.2°, 47.3°, 54.5°, 60.5°, which are the diffractions of $Si_{2}Te_{3}$ with the indices of (112), (114), (006), (116), (008), and (118), respectively (JCPDF 00-022-1323). The (112) diffraction peak for the nanowires is stronger than other peaks because the random orientation of the nanowires. However, the (004) peak is the strongest one in the XRD pattern of the nanoplates, which clearly indicates the growth direction of (001), i.e. layer by layer growth. No diffraction peaks from other materials were observed in the nanoplates, indicating of pure phase of Si₂Te₃ materials. The XRD measurements confirm that the obtained nanoplates and nanowires are Si_2Te_3 with trigonal structure (space group $P\bar{3}1c$).

Figure 3b shows the Raman spectra of the Si_2Te_3 nanoplates and nanowires. The Si_2Te_3 nanoplate shows a very strong peak at 138 cm⁻¹ and one relatively weak peak located at 326 cm⁻¹, which are respectively assigned to A_{1g} and E_g modes. The nanowire shows a very similar spectrum as that of horizontal nanoplates except that the E_g mode is hard to see due to noise. The Raman data of Si_2Te_3 nanostructures are in good agreement with the previous reports [1, 26].

The vertical nanoplates may be explained by vapor–solid growth model because of the importance of solid–solid interface as reported by Keuleyan et al. [1]. The flat $\mathrm{Si}_2\mathrm{Te}_3$ nanoplates may be due to the growth mechanism of VLS. The process of growth is illustrated as follows. Te at the center of the furnace vaporizes first because its lower vaporization point ($\mathrm{T}_m = 450~^{\circ}\mathrm{C}$) and condenses on the substrate as initial nucleation sites, on which the Si react with Te to form

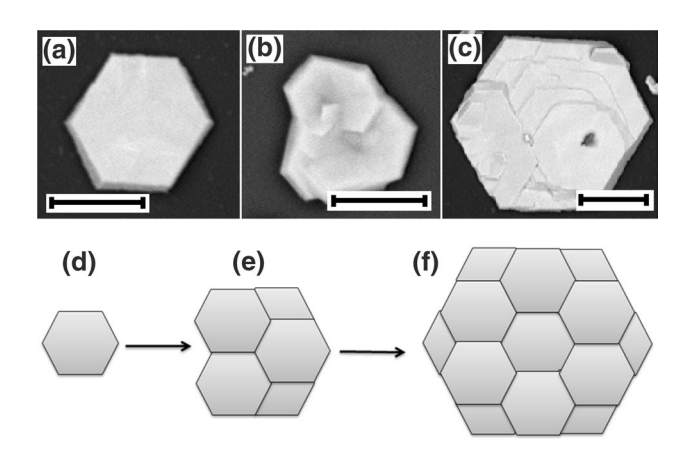
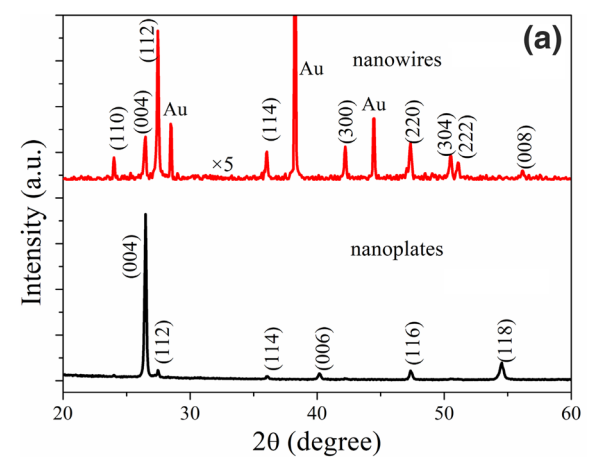


Fig. 4 a–c SEM images of growth process of Si_2Te_3 microplates. d–f Schematic diagram of growth mechanism of Si_2Te_3 microplate. Scale bars are a 2 μ m; b 5 μ m; and c 5 μ m

Si₂Te₃. Figure 4 shows the evolution of Si₂Te₃ microplates at different stages, i.e. grown for different times and the corresponding schematic diagrams. It can be seen that the nanoplates may be formed initially and additional nanoplates also grown adjacent to the previous. As more nanoplates stack on each other, the microplate is formed as illustrated in Fig. 4d–f.

The Si₂Te₃ NWs grown at different substrate temperatures as shown in Fig. 2a, b suggest that the morphology of Si₂Te₃ changes from nanotaper to nanowire as the substrate temperature increases. This phenomenon may be explained as following: In the VLS growth method, liquid nanosized droplets are formed on a substrate via an eutectic reaction between Au nanoparticles and the Si₂Te₃ solutes provided from vapor-phase precursors in the CVD system. The continued feeding of the Si₂Te₃ reactants into the liquid droplets supersaturates the eutectic which leads to nucleation of the solid semiconductor. The solid/liquid



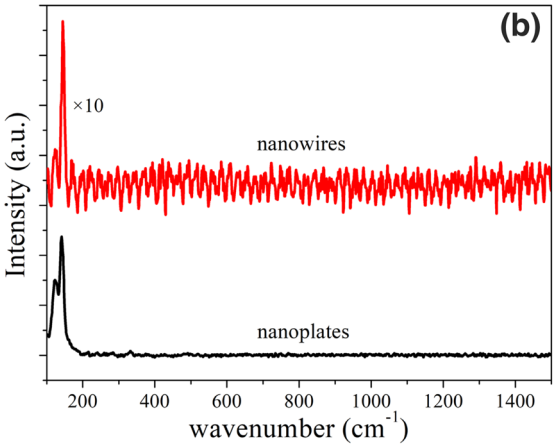


Fig. 3 a XRD patterns nanoplates and nanowires. b Raman spectra of nanoplates and nanowires



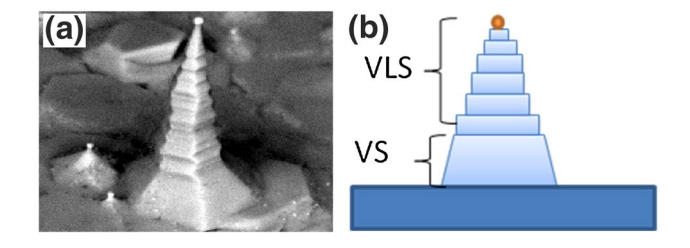


Fig. 5 a SEM image and b schematic diagram of growth mechanism of a Si_2Te_3 nanotaper

interface forms the growth interface, which acts as a sink. The continued semiconductor incorporates into the interface to form the nanowires and the Au droplets are on the top [29]. In fact, there are two competing interfaces during the nanowire growth, i.e. the liquid/solid interface between the eutectic and the nanowire and the gas/solid interface between the reactants and the exposed surface of the growing nanowire. The first interface results in the VLS growth and axial elongation of the nanowires while the second interface results in VS growth and thickening the nanowires in the radial direction. Both mechanisms depend on the growth condition such as the pressure, flow rate, temperature and ratio of reactant species. For example, Dayeh et al. [30], investigated the InAs nanowires grown with different As/In (V/III) ratio. They found that the growth mode changed from VS to VLS with the decrease of V/III ratio, i.e. VS growth is over VLS growth at higher V/III ratio. During our experiment, the Te/Si ratio changes with both the growth time and temperature. At low substrate temperature, growth of the Si₂Te₃ nanotapers is favored due to the high Te/Si ratio because Te has low vaporization point, which leads to a growth by VS over VLS. However, the VLS growth gradually dominates as the Te/ Si ratio decreases at high temperature, which results in the growth of nanowires. It should be pointed out that the temperature affects the vapor pressure of Si and Te in the growth chamber, and therefore influences the growth mode. However, the composition of the obtained materials may not be affected as being observed in the growth InAs. Further study is being performed to look into the details.

Figure 5 shows the SEM image of tapered shape $\mathrm{Si}_2\mathrm{Te}_3$ nanostructure and its schematic diagram of growth mechanism. This is a combination of VS and VLS growth. In the initial growth of the $\mathrm{Si}_2\mathrm{Te}_3$ nanotapers, the morphology shows pyramid shape, which is due to VS growth model [31, 32]. In the following growth process, the VS is then replaced by VLS mode. The taper-shape $\mathrm{Si}_2\mathrm{Te}_3$ is composed of nanoplates with much small size and usually limited by the catalysts.

4 Conclusions

In summary, Si_2Te_3 nanoplates, microplates, nanotapers and nanowires were synthesized via a chemical vapor deposition method. It was found that catalyst Au, substrate temperature and growth time played an important role in the synthesis of Si_2Te_3 . Si_2Te_3 nanotapers and nanowires are obtained with Au as catalysts, while only nanoplates and microplates are obtained with catalyst free substrates. Substrate temperature affects the size of Si_2Te_3 nanoplate, which increases with the decrease of temperature. The growth time also affects the morphology of the Si_2Te_3 nanostructures. The growth mechanism of microplates is due to Te self-catalyzed VLS while the nanotaper is a result of growth switch from VS to VLS mode.

Acknowledgements Keyue Wu gratefully acknowledges the scholarship support from the Educational Commission of Anhui Province of China. This work was partially supported by Natural Science foundation of Educational Commission of Anhui Province of China (KJ2015A150), National Natural Science Foundation of China (21377099), and National Science Foundation (1709528).

References

- S. Keuleyan, M. Wang, F.R. Chung, J. Commons, K.J. Koski, Nano Lett. 15, 2285–2290 (2015)
- K. Ploog, W. Stetter, A. Nowitzki, E. Schonherr. Mater. Res. Bull. 11, 1147 (1976)
- 3. A. Weiss, A. Z. Weiss. Anorg. Allg. Chem. 273, 124 (1953)
- A.P. Lambros, N.A. Economou, Phys. Status Solidi B 57, 793 (1973)
- 5. U. Zwick, K.H. Rieder, Z. Phys. B 25, 319 (1976)
- 6. K. Ziegler, U. Birkholz, Phys. Status Solidi A 39, 467 (1977)
- G. Gregoriades, G.L. Bleris, J. Stoemenos, Acta Cryst. B. 39, 421–426 (1983)
- A.P. Lambros, N.A. Economou, phys. stat. sol. (b) 57, 793–799 (1973)
- X. Shen, Y.S. Puzyrev, C. Combs, S.T. Pantelides, Appl. Phys. Lett. 109, 113104–113108 (2016)
- R. Juneja, T. Pandey, A.K. Singh, Chem. Mater. 29, 3723–3730 (2017)
- S. Steinberg, R.P. Stoffel, R. Dronskowski, Cryst. Grow. Des. 16, 6152–6155 (2016)
- R. Mishra, P.K. Mishra, S. Phapale, P.D. Babu, P.U. Sastry, G. Ravikumar, A.K. Yadav, J. Solid State Chem. 237, 234–241 (2016)
- B.Z. Tian, X.L. Zheng, T.J. Kempa, Y. Fang, N.F. Yu, G.H. Yu,
 J.L. Huang, C.M. Lieber, Nature 449, 885–889 (2007)
- E. Shalev, E. Oksenberg, K. Rechav, R.P. Biro, E. Joselevich, ACS Nano. 11, 213–220 (2017)
- F. Qian, Y. Li, S. Gradecak, D.L. Wang, C.J. Barrelet, C.M. Lieber, Nano Lett. 4, 1975–1979 (2004)
- Y. Cui, D. van Dam, S.A. Mann, N.J.J. van Hoof, P.J. van Veldhoven, E.C. Garnett, Nano Lett. 16, 6467 6471 (2016). E. P. A. M. Bakkers, and J. E. M. Haverkort
- X.T. Cao, X. Cao, H.J. Guo, T. Li, Y. Jie, N. Wang, Z.L. Wang, ACS Nano 10, 8038–8044 (2016)



- Y.M. Brovman, J.P. Small, Y. Hu, Y. Fang, C.M. Lieber, J. Appl. Phys. 119, 234304 (2016)
- C.-H. Chien, P.-C. Lee, W.-H. Tsai, C.-H. Lin, C.-H. Lee, Y.-Y. Chen, Sci. Rep. 6, 23672 (2016)
- N. Kornienko, N.A. Gibson, H. Zhang, S.W. Eaton, Y. Yu, S. Aloni, S.R. Leone, P. Yang, ACS Nano 10, 5525–5535 (2016)
- K.S. Novoselov, A.K. Geim, S.V. Morozov, D. Jiang, Y. Zhang, S.V. Dubonos, I.V. Grigorieva, A.A. Firsov, Science 306, 666–669 (2004)
- X. Geng, W. vSun, W. Wu, B. Chen, A.A. Hilo, M. Benamara, H. Zhu, F. Watanabe, J. Cui, T. Chen, Nat. Commun. 7, 10672 (2016)
- 23. T. Niu, Nanotoday **12**, 7–9 (2017)
- R. Agarwal, C.J. Barrelet, C.M. Lieber, Nano Lett. 5, 917–923 (2005)

- R.X. Yan, J.H. Park, Y. Choi, C.J. Heo, S.M. Yang, L.P. Lee, P.D. Yang, Nat. Nanotechnol. 7, 191–196 (2012)
- K.Y. Wu, W.W. Sun, Y. Jiang, J.Y. Chen, L. Li, C.B. Cao, S.W. Shi, X. Shen, J.B. Cui, J. Appl. Phys. 122, 075701–075708 (2017)
- P. Nguyen, H.T. Ng, T. Yamada, M.K. Smith, J. Li, J. Han, M. Meyyappan, Nano Lett. 4, 651–657 (2004)
- V.G. Dubrovskii, G.E. Cirlin, N.V. Sibirev, F. Jabeen, J.C. Harmand, P. Werner, Nano Lett. 11, 1247–1253 (2011)
- 29. W. Lu, C.M. Lieber, J. Phys. D 39, R387-R406 (2006)
- 30. S.A. Dayeh, E.T. Yu, D.L. Wang, Nano Lett. 7, 2486–2490 (2007)
- J.C. Shin, D.Y. Kim, A. Lee, H.J. Kim, J.H. Kim, W.J. Choi, H.S. Kim, K.J. Choi, J. Cryst. Growth 372, 15–18 (2013)
- K.A. Dick, K. Deppert, T. Martensson, B. Mandl, L. Samuelson, W. Seifert, Nano Lett. 5, 761–764 (2005)

